IEEE Photonics Journal
An IEEE Photonics Society Publication

Open Access

Distributed Temperature/Vibration Fiber Optic Sensor With High Precision and Wide Bandwidth

Volume 11, Number 6, December 2019

Tao He
Yanli Ran
Tao Liu
Hao Li
Cunzheng Fan
Wei Zhou
Zhijun Yan
Deming Liu
Qizhen Sun

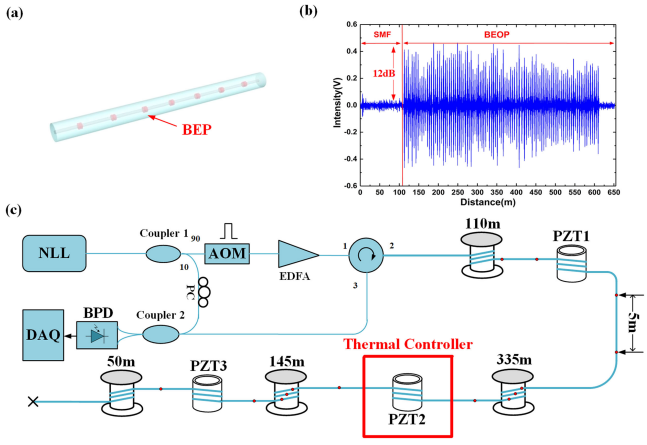

DOI: 10.1109/JPHOT.2019.2951733

Distributed Temperature/Vibration Fiber Optic Sensor With High Precision and Wide Bandwidth

Tao He [1,2] Yanli Ran [1,2] Tao Liu, Hao Li [2] Cunzheng Fan,[2] Wei Zhou,[2] Zhijun Yan [2] Deming Liu,[2] and Qizhen Sun [2]

[1]Institute of Microscale Optoelectronics (IMO), Shenzhen University, Shenzhen 518060, China
[2]School of Optical and Electronic Information, Wuhan National Laboratory for Optoelectronics, and National Engineering Laboratory for Next Generation Internet Access System, Huazhong University of Science and Technology, Wuhan 430074, China

DOI:10.1109/JPHOT.2019.2951733

Manuscript received September 12, 2019; revised October 25, 2019; accepted November 1, 2019. Date of publication November 6, 2019; date of current version November 13, 2019. This work was supported in part by the National Key Research and Development Program of China under Grant 2018YFB2100902, in part by the Wuhan Science and Technology Bureau Achievement Conversion Project under Grant 2018010403011330, in part by the Fundamental Research Funds for the Central Universities under Grant 2019kfyRCPY095. Corresponding author: Yanli Ran (e-mail: ylran@szu.edu.cn).

Abstract: Distributed fiber optic sensor for multi-parameter measurements plays a crucial role in various applications. In this work, distributed temperature/vibration fiber optic sensor with high precision and wide bandwidth is proposed and experimentally demonstrated. To improve the signal-to-noise ratio (SNR) and sensitivity of the system, the backscattering enhanced optical fiber (BEOF) is employed to provide strong and stable sensing signal. With the assistance of the coherent phase detection, a high precision measurement of phase can be achieved. In addition, the wavelet packet decomposition algorithm is put forward to effectively discriminate the quasi-static temperature and dynamic vibration signals. In the experiment, wide bandwidth vibration signal from 0.01 Hz to 20 kHz can be successfully detected. Owing to the high sensitivity of the system, the local temperature change within the range of only 10 cm can be captured with high precision of 0.095 °C. Besides, the system has a good capability of fast response to the external temperature variation where the response time is around 0.3 seconds, which is meaningful for the early warning of centimeters-level sized fire source in the special oil and gas pipelines monitoring applications.

Index Terms: Optical sensors, distributed measurement, temperature/vibration, back-scattering, phase modulation and wavelet packet decomposition.

1. Introduction

Integration of distributed temperature and vibration fiber optic sensing systems are becoming a pressing requirement in the industrial infrastructure monitoring [1], [2]. Especially in the oil and gas pipelines security monitoring applications, the function of distributed temperature detection of small region, early warning of explosion or fire disaster as well as a wide vibration response bandwidth is vitally important. Raman scattering-based optical time domain reflectometry (OTDR) sensors [3] can achieve the distributed temperature measurement with meter-scale spatial resolution, while thermally-activated spontaneous Raman scattering light is not sensitive to the external strain. And the low sensitivity makes it difficult for monitoring a centimeters-scale fire source. Besides,

the Brillouin scattering-based OTDR system [4] can realize distributed temperature and strain measurement by combining the intensity and frequency shift of Brillouin backscattering. L. Q. Luo *et al*. have reported a high accuracy distributed temperature and strain sensor based on B-OTDR with an accuracy of 0.43 °C and 10 $\mu\varepsilon$, respectively [5]. Whereas the demodulation method requires frequency-sweep processing which results in a low demodulation rate. Hence, the bandwidth of vibration sensing is limited. Recently, the phase-sensitive optical time domain reflectometry (φ-OTDR) sensors based on Rayleigh scattering light have drawn a lot of research interest owing to its fast response and high sensitivity to external perturbations [6], [7]. And the sensor system is able to detect dynamic strain with kHz-level frequency band. Unfortunately, due to a weak amplitude and a randomly distributed position of Rayleigh scattering (RS) light in normal single mode fiber (SMF), the precision and SNR of signal are seriously affected. Thus, the detection of sub-Hz level signal is greatly degraded by the low frequency phase noise induced by unstable RS signal [8]. And it is not suitable for the measurement of quasi-static temperature and ultra-low frequency vibration change.

Moreover, some hybrid systems for simultaneous measurements of static temperature and dynamic vibration have been demonstrated. Jing Dong Zhang *et al*. realized up to 4.8 kHz vibration sensing with 3 m spatial resolution and the accuracy of 2 °C temperature measurement along the 10 km SMF with 80 cm spatial resolution through the combination of φ-OTDR and B-OTDR fiber-optic system [9]. Yonas Muanenda *et al*. integrated φ-OTDR with R-OTDR to achieve the up to 500 Hz vibration detection and the temperature resolution of 0.5 °C at 5 km SMF with 5 m spatial resolution [10]. Yet these sensors could not meet requirement for accurate measurement of temperature in some special security monitoring applications. Besides, the integration of these techniques undoubtedly adds a significant increase in the cost and complexity of the system.

And some high precision distributed fiber sensors for temperature and strain sensing have attracted a wide attention. Yahei Koyamada *et al*. achieved distributed temperature and strain measurements with a high resolution of 0.01° C/0.1 $\mu\varepsilon$ in 8-km-long fiber with spatial resolution of 1 m by using coherent OTDR with a precisely frequency-controlled light source [11]. Additionally, by mean of the measurements of local birefringence and local φ-OTDR frequency shift, a distributed temperature and strain sensor with high precision of 0.04 °C/0.5 $\mu\varepsilon$ along a 100 m-long polarization maintaining fiber has been experimentally demonstrated [12]. Although these methods have an advantage in high precision measurement of temperature, it is difficult to realize the kHz-level vibration measurement due to a frequency-sweep processing in the demodulation. In addition, on the base of requirement of national standards for some special oil pipelines monitoring, temperature detector must be capable of a small scale of fire source response less than 10 cm because most accidents occur on the local area of oil pipelines or tunnels. However, the above technologies have defects in the realization of centimeters-scale fire source detection with high precision. Accordingly, the research of centimeters-scale fire source detection with high precision and wide bandwidth frequency response is a significant work.

In this paper, simultaneously distributed temperature/vibration fiber optic sensor based on φ-OTDR principle combined with the backscattering enhanced optical fiber (BEOF) is proposed and experimentally demonstrated. In order to improve the SNR and sensitivity of the system, the random fluctuant and weak RS in the SMF is replaced by stable and strong back-scattering signals generated by backscattering enhanced points (BEPs) along the longitudinal direction of the fiber, which is named as BEOF. Thus, external perturbations exerted on short fiber length of centimeters-level can be detected due to the high sensitivity. Not only quasi-static signals but also kHz-level high frequency signals can be high-fidelity recovered by high stable phase demodulation. Furtherly, the phase variation induced by the temperature and vibration can be discriminated via the wavelet packet decomposition algorithm to realize simultaneously distributed measurement of temperature and vibration. Finally, verification experiments are performed to verify a wide-band frequency response from 0.01 Hz to 20 kHz. And temperature variation applied on short fiber length of only 10 cm can be successfully captured with high precision of 0.095 °C and fast response time approximately 0.3 seconds.

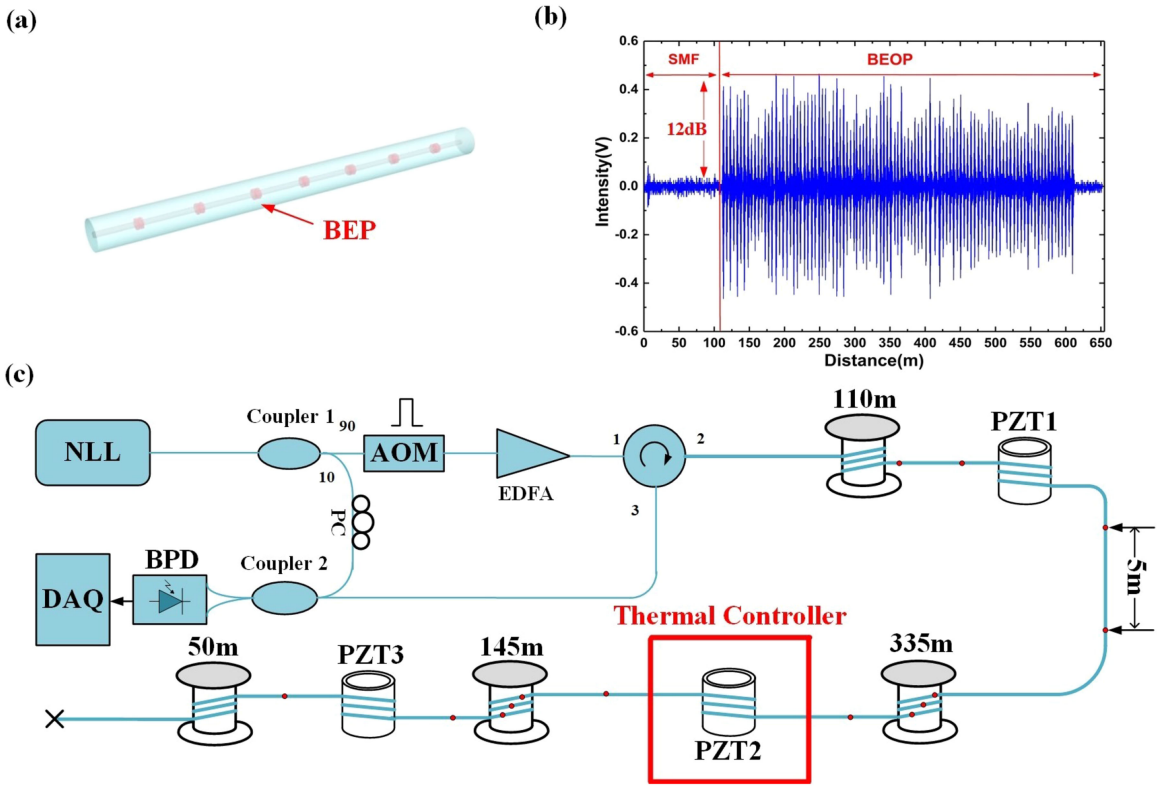

Fig. 1. (a) The BEPs along the longitudinal direction of the BEOF. (b) A backscattering trace of the sensing fiber which contains SMF and BEOF. (c) System configuration of the distributed temperature and vibration sensor; NLL: Narrow Linewidth Laser; PC: Polarization Controller; AOM: Acousto-Optic Modulator; EDFA: Erbium-Doped Fiber Amplifier; PZT: Piezoelectric Transducer; BPD: Balanced Photo Detector; DAQ: Data Acquisition Card.

2. Principle

2.1 System Configuration

In a coherent detection system, the interference between multiple weak scatters within one pulse width would cause to the randomness of the backscattered light when a high coherence pulse injecting into normal single mode fiber (SMF), which decreases the SNR of the backscattered trace and leads to random intensity fading. To improve the SNR and measurement precision of the system, the BEOF is applied [13]. The BEOF contains a series of consecutive backscattering enhanced points (BEPs) as shown red dots in Fig. 1(a), which is fabricated by laser exposure processing along the longitudinal direction of fiber. Due to the BEPs with a much stronger backscattering coefficient, the intensity of the backscattered light from the BEPs is greatly enhanced. In experiment, the sensing BEOF fiber is consisted of 101 BEPs with 5 m space interval. Form Fig. 1(b), it can be seen that compared with the intrinsic Rayleigh scattered (RS) light from SMF, the backscattered intensity of BEPs is increased by 12dB at local positions. Besides, the backscattered signal of BEOF has a stable distribution owing that there is no overlap and interference between the signals from adjacent BEPs. Consequently, these BEPs are a promising candidate for the sensing points to improve the SNR of sensor system.

The schematic of the distributed temperature and vibration sensing system is shown in Fig. 1(c). A high coherent narrow line-width (less than 1 kHz) laser with 20 mW continuous output at 1550.12 nm is used as the optical source. The continuous light is divided into two parts by a 90:10 coupler 1. The 10% port goes through the polarization controller (PC) to eliminate the effect of polarization

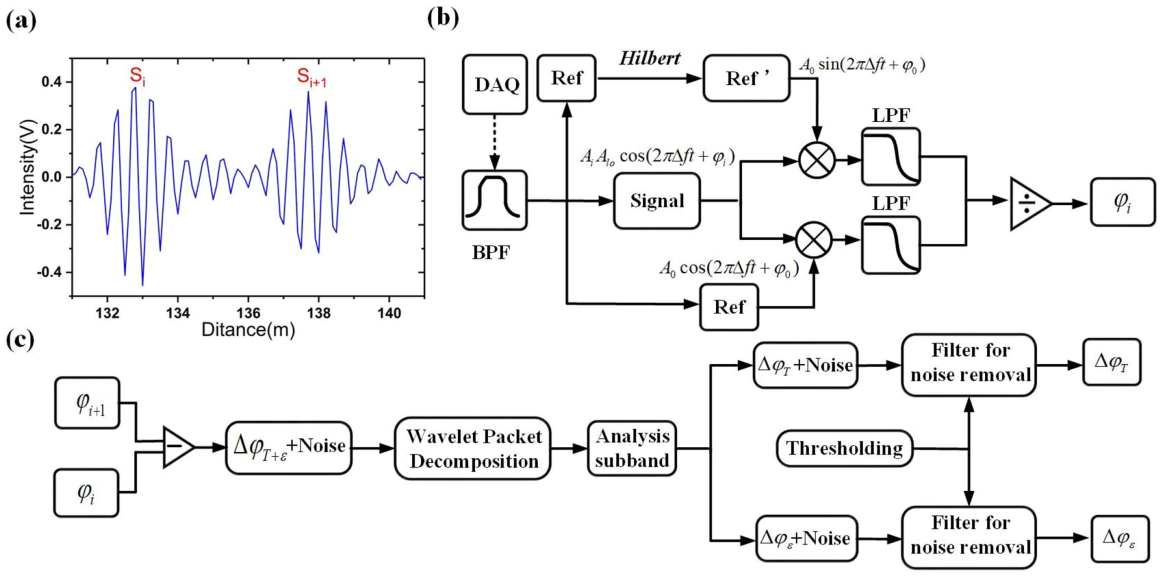

Fig. 2. (a) Beat frequency signals. (b) Phase demodulation. (c) temperature-vibration discrimination algorithm schematic diagram.

dependent fading by adjusting the polarization state of the local-oscillator (LO) light. The 90% part from coupler 1 is modulated into pulses with duration time of 20 ns by the acoustical optical modulator (AOM) to impose a 200 MHz frequency shift from the original optical frequency. While the sensing system sampling rate depends on the repetition rate of light pulse. Hence, the repetition rate of light pulse varies according to practical measurement requirements. After amplified by an erbium-doped optical fiber amplifier (EDFA), the probe pulses launch into the sensing fiber with length of 650 m through a circulator. Next, the steadily enhanced backscattering signal from each BEP is carried with the information of external temperature and dynamic strain and interferes with the local-oscillator light at the 50:50 coupler. The AC component of the generated beat frequency signal is detected by a balanced photo detector (PBD480C-AC, Thorlabs). Then the electrical signal is recorded by a data acquisition card (DAQ) with a sample rate of 2 GS/s. Finally, the raw data is transmitted to a computer for further process.

2.2 System Demodulation Process

To get the higher optical gain and effectively reduce the detection noise, the coherent detection method is involved [14]. The backscattering light from the BEPs combines with the LO light to form the beat frequency signal as shown in Fig. 2(a). The detected current of the *i*-th beat frequency signal $I_{si}(t)$ can be expressed as:

$$I_{si}(t) = A_i A_{lo} \cos(2\pi \Delta f t + \varphi_i) \tag{1}$$

where A_i and A_{lo} are the amplitude of the scattered light from *i*-th BEP and LO, respectively. $\Delta f = 200$ MHz is the frequency shift of the probe pulse, which is generated by AOM. And φ_i is the phase difference between the scattered light from *i*-th BEP and LO.

The phase demodulation algorithm is illustrated in Fig. 2(b). The raw data obtained by DAQ passes through a bandpass filter (BPF) with center frequency at 200 MHz to eliminate the phase noise. Further, a pair of orthogonal reference functions can be obtained by Hibert transform. After multiplying the beat frequency signal, another pair of orthogonal functions about φ_i is generated. According to the product to sum formula and the I/Q demodulation [15], φ_i from the *i*-th BEP can be calculated. Similarly, φ_{i+1} can be also got. Consequently, the phase variation between the *i*-th BEP

and $(i+1)$-th BEP can be given as:

$$\Delta\varphi = \varphi_{i+1} - \varphi_i \tag{2}$$

Thus, the phase variation between every two adjacent BEP can be calculated to realize the distributed measurement. The optical path difference of a length of L fiber between two adjacent BEP would change when encountering a temperature variation of ΔT or a dynamic strain of $\Delta\varepsilon$ [16], resulting in a phase variation $\Delta\varphi_{T+\varepsilon}$, which can be expressed as:

$$\Delta\varphi_{T+\varepsilon} = \Delta\varphi_T + \Delta\varphi_\varepsilon \frac{4\pi n}{\lambda}\left[\left(L\frac{\partial n}{\partial T} + n\frac{\partial n}{\partial T}\right)\Delta T + \left(L\frac{\partial n}{\partial \varepsilon} + n\frac{\partial L}{\partial \varepsilon}\right)\Delta\varepsilon\right] \tag{3}$$

Where $\Delta\varphi_T$, $\Delta\varphi_\varepsilon$ corresponds to the change of phase induced by temperature and dynamic strain separately, L is the length of the fiber under test. Yet, the phase variation is susceptible to external perturbation induced both temperature and dynamic strain. Hence, an effective method of temperature-vibration discrimination is proposed and shown in Fig. 2(c). Actually, phase variation $\Delta\varphi_{T+\varepsilon}$ involved with the ambient noise affects the measurement accuracy of temperature and vibration directly. In order to filter out the noise effectively, signals are split into different frequency section by wavelet packet decomposition method. On the one hand, the properties of the wavelet packet coefficients of the effective signal and noise is different. The effective signal is mainly concentrated in a few wavelet packet coefficients with large amplitude while the noise is distributed in the whole wavelet domain. On the other hand, the quasi static temperature change and fast vibration events generally occupy different frequency response band. After the analysis sub-band, the quasi-static temperature and dynamic vibration signals can be extracted from low pass and high pass band. And the noise can be restrained via thresholding operation, finally, temperature and vibration signals can be well reconstructed to realize temperature-vibration simultaneous measurement.

According to the Equation (3), for the purposes of the quasi-static temperature measurements only the thermal coefficient γ is considered, which can be presented as follows:

$$\gamma = \left(\frac{1}{n}\frac{\partial n}{\partial T} + \frac{1}{L}\frac{\partial L}{\partial T}\right) \tag{4}$$

It is comprised of a thermo-optic coefficient and a thermal expansion coefficient. Assuming $\gamma = 9.15 \cdot 10^{-6}(^{\circ}C^{-1})$ given by [17] and $\lambda = 1550$ nm, $n = 1.467$, $\Delta\varphi_T$ for the ΔT variation applied on a L length fiber can be given as:

$$\Delta\varphi_T = 108.825(rad/m\cdot^{\circ}C) \cdot L \cdot \Delta T \tag{5}$$

On the basis of the formula (5), the induced phase variation $\Delta\varphi_T$ is about 10.883 rad when 1 °C temperature change is applied on the fiber length of 10 cm. With the strong and stable signal from BEOF and high-sensitivity of the system, the local temperature variation within the range of only 10 cm can be captured with high precision. The follow experiments have been implemented to verify the system performance of the distributed temperature and vibration simultaneous measurement with fast response speed and broadband frequency response.

3. Results

3.1 Simultaneous Measurement of Temperature and Vibration

In order to corroborate the feasibility of temperature-vibration simultaneous measurement, 1 m long fiber under test (FUT) is coiled around a Piezoelectric Transducer (PZT) within the thermal controller located at 451 m as shown in Fig. 1(c). Next, the temperature of the thermal controller starts to rise and the PZT is driven by a 200 Hz sine-wave generated from the function waveform generator. The phase variation induced by the heating and vibration can be detected by this system with a sampling rate of 4 kHz drawn as a rad curve in Fig. 3(a). Besides, a blue curve presents the phase variation of FUT in air without heating and vibration. Obviously, it can be seen from the enlarged part of Fig. 3(a) that the sinusoidal shape waveform corresponds to the vibration-disturbance from the PZT and the

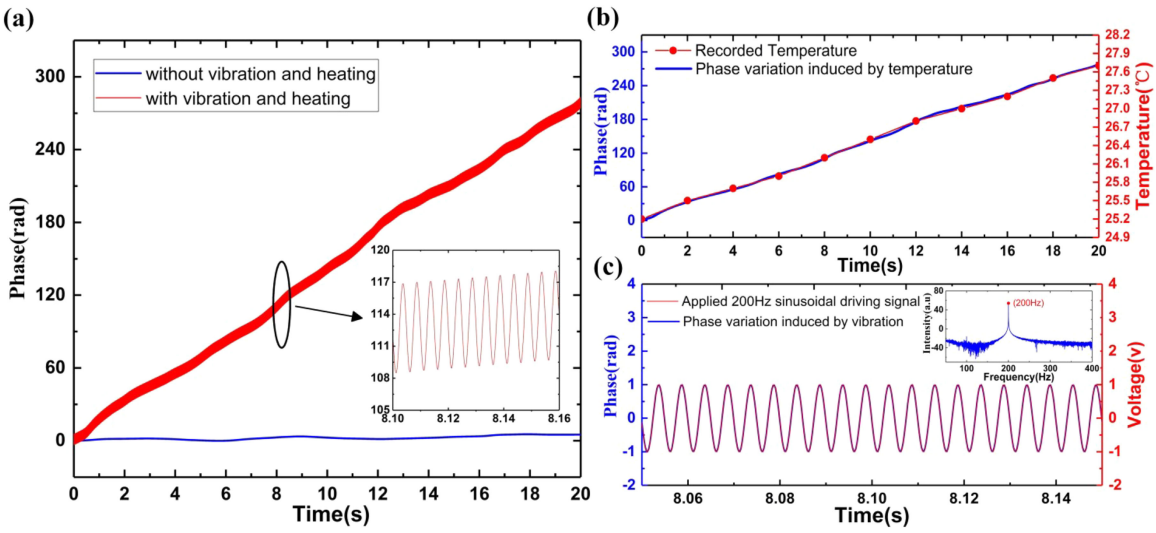

Fig. 3. (a) Phase variation of a FUT induced by heating and vibration and it in air without heating and vibration. (b) Phase variation of a FUT induced by temperature. (c) Phase variation of a FUT induced by vibration.

inclined part of waveform corresponds to the temperature-disturbance from the thermal controller. Then, by the means of the wavelet packet decomposition algorithm mentioned above, the phase variation induced by the temperature and vibration can be separately derived and given in Fig. 3(b) and Fig. 3(c). As shown in Fig. 3(b), the red points represent the recorded temperature during the process of heating. The demodulated phase variation as the blue curve is found to be closer to the temperature change. Besides, Fig. 3(c) shows a waveform comparison of the demodulated vibration signal and applied sinusoidal driving signal after the normalizing process, which is consistent and undistorted. And the power spectrum of demodulated vibration signal, where the frequency respond peak is at 200 Hz, is shown in the inset of Fig. 3(c). As a result, the system possesses an excellent performance for temperature and vibration simultaneous measurement.

3.2 Distributed and Wideband Vibration Sensing

In the vibration measurement, three PZTs wrapped with 1 m fiber are placed at the distance of 116 m, 451 m and 596 m along the sensing fiber respectively as three vibration sources. Additionally, the frequency and amplitude of signal can be controlled by a function waveform generator and the vibration of the PZT can be transmitted to the fiber under test. According, PZT1, PZT2 and PZT3 are separately driven by 10 Hz sine-wave of 3 V, 500 Hz sine-wave of 2.5 V and 5 kHz sine-wave of 1.5 V from the three signal channels of the function waveform generator. When a sampling rate of sensor system is set to 60 kHz, the waveform and location information of the multi-point vibration events can be distinctly observed in Fig. 4. There are three simultaneous vibrations at the distance of 115 m, 450 m, 595 m, and they are shown as green line, blue line and red line separately.

As shown in Fig. 5(a), (c), (e), the waveform comparison of the measured vibration signals and the standard sine wave with 10 Hz, 500 Hz and 5 kHz. Apparently, the waveform of demodulated signals is regular and basically consistent with the standard signals. Further, the fidelity of the demodulation system is evaluated by the waveform maximum error. The maximum error is defined by the maximum deviation value of the two waveforms which have been normalized. As shown in the inset of Fig. 5(a), (c), (e), the maximum errors of three measured signals are 0.7%, 1.25% and 3.97%, respectively. Besides, their power spectrums are severally depicted in Fig. 5(b), (d), (f). It is worth to mention that all of the three demodulated signals have high SNR over 61.8 dB. Thus,

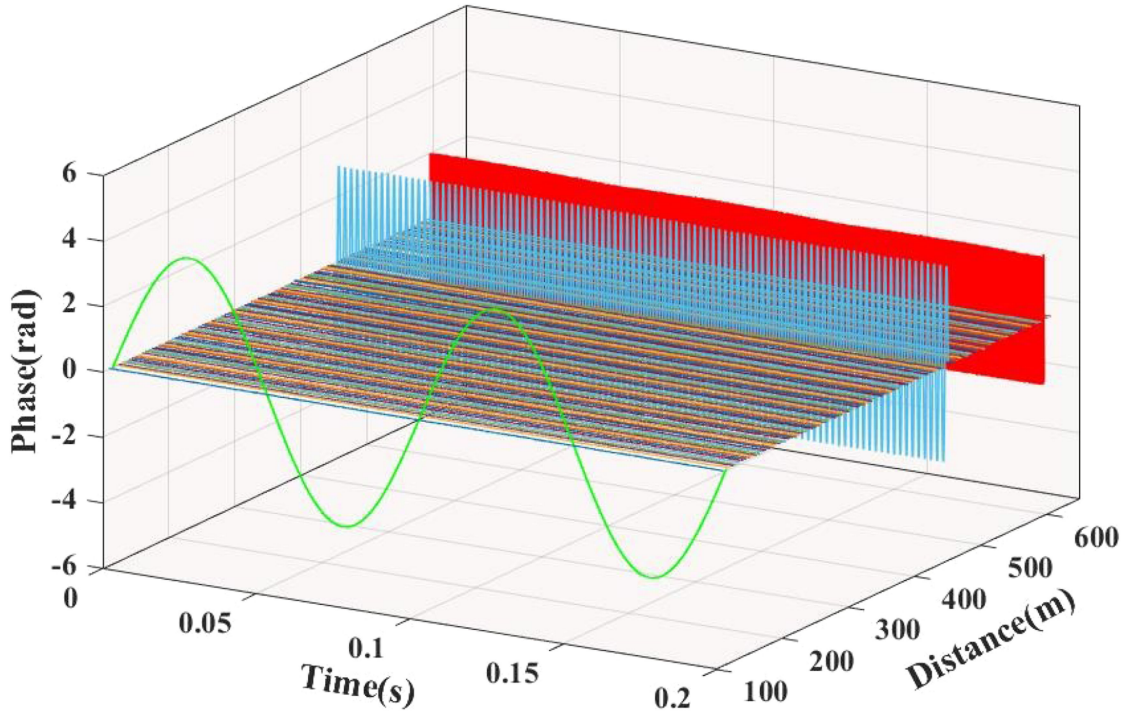

Fig. 4. The waveform of demodulated signals distribution along the sensing fiber.

the results indicate that the demodulated system has a capability of high-fidelity waveform recovery except for high SNR.

To verify the detection capability of ultra-low frequency signals of system, the function generator provides an ultra-low frequency sinusoidal signal of 0.01 Hz for PZT which is wrapped with 1 m fiber and located at the distance of 601 m. The 0.01 Hz ultra-low frequency sinusoidal waveform is demodulated and drawn in Fig. 6(a), which is regular and less distorted. On the other hand, the PZT is excited by different frequency sinusoidal signals from 0.01 Hz to 20 kHz to demonstrate the detection performance of wide frequency bandwidth signals, as shown in Fig. 6(b), in which X-axis uses a base-10 logarithmic coordinate to make the frequency-spaced look evenly. It is remarkable that a wide frequency from 0.01 Hz to 20 kHz vibration signals is detected successfully by this system.

3.3 Distributed and High Precision Temperature Sensing

Attesting to the feasibility of the distributed temperature measurement, three segments FUT of 10 cm are located at the distance of 151 m, 376 m and 599 m along the whole sensing fiber respectively, which are applied on different temperature variations. After a few minutes, the temperature of the first segment of FUT rises from 25.12 °C to 97.83 °C. Meanwhile, temperature of the second segment of FUT rises from 25.23 °C to 51.71 °C and then falls to 26.39 °C. While temperature of the third segment of FUT falls from 71.21 °C to 31.13 °C. The temperature color map is shown in Fig. 7(a), in which the x-axis is the location of the FUT and y-axis is the recording time. As it shown in the figure, three clearly phase variation zones are framed as ‘a’, ‘b’ and ‘c’ dotted boxes and located at 150m, 375 m and 600 m, respectively, which are the same as the position of applied temperature variations. According to the results, the phase value within zone ‘a’ is straightly increased as the temperature rising, and the phase value within zone ‘b’ first increases and then decreases. Besides, the phase value in zone ‘c’ is sharply declined. Obviously, the phase variation induced by the temperature change is consistent with the fluctuation tendency of temperature. Whereas the phase variation

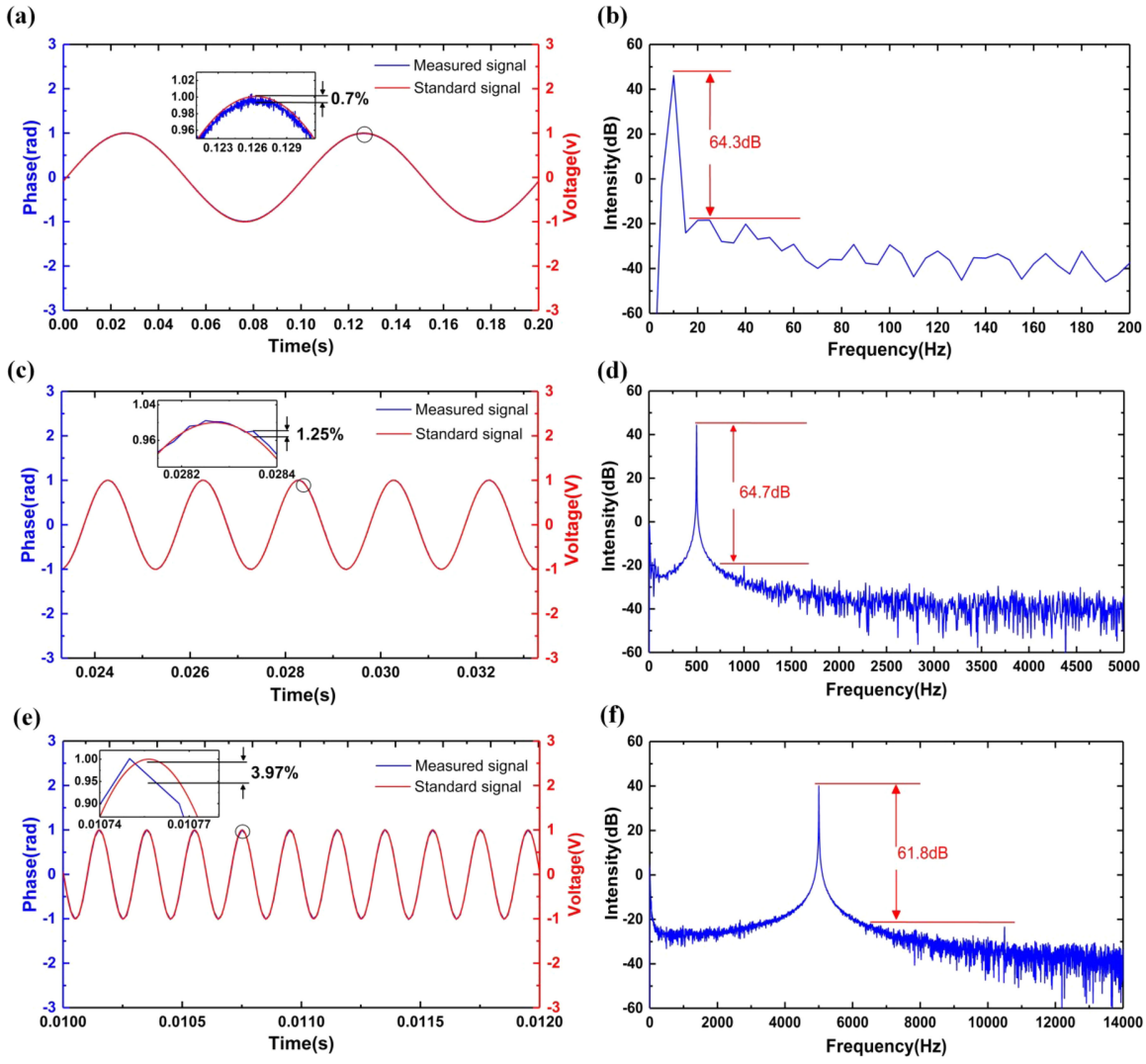

Fig. 5. The waveform comparison between measured signal and standard signal of (a) 10 Hz; (c) 500 Hz; (e) 5 kHz; Power spectrums of measured signals (b) 10 Hz; (d) 500 Hz; (f) 5 kHz.

of the non-affected region is almost zero. And the experiment indicates that temperature variation applied on short fiber length of only 10 cm can be successfully detected.

In order to get temperature sensitivity of the system for 10 cm FUT, the temperature of 10 cm FUT is controlled by the super-high precision thermal controller with a temperature accuracy of ±0.001 °C. Then the temperature would be gradually risen from room temperature of 23.851 °C with 5 °C temperature increment, and the phase variation corresponding to temperature varying is recorded as shown blue dots in Fig. 7(b). Accordingly, the relationship between the phase variation and temperature change is obtained by the linear fitting and the result shows a good linear response of 10.979 rad/°C for 10 cm FUT. Meanwhile, the phase fluctuation of a 5 m long reference fiber (separation of BEPs is 5 m) is measured by placing the fiber in the commercial insulating box at 25 °C for 750 seconds, which has a thermal and airflow insolation function and the temperature is controlled by the Thermo Electric Cooler (SLD70-SN9RDA) with a temperature accuracy of ±0.001 °C. Then the recorded maximum phase fluctuation of reference fiber is around 1.04 rad, which is shown as the green line in Fig. 7(b). Finally, the temperature precision could be calculated

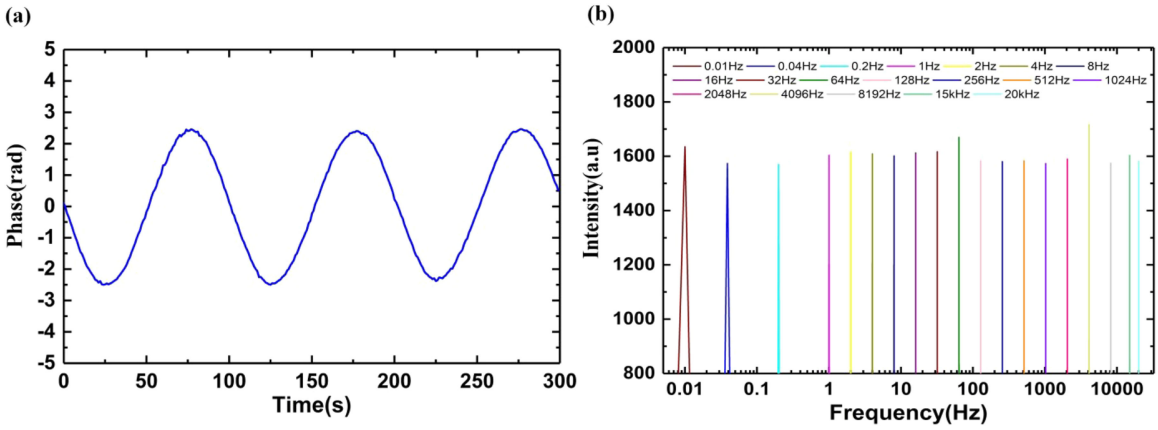

Fig. 6. (a) The ultra-low frequency measured signal waveform of 0.01 Hz. (b) Power spectra of wide frequency vibrations from 0.01 Hz to 20 kHz.

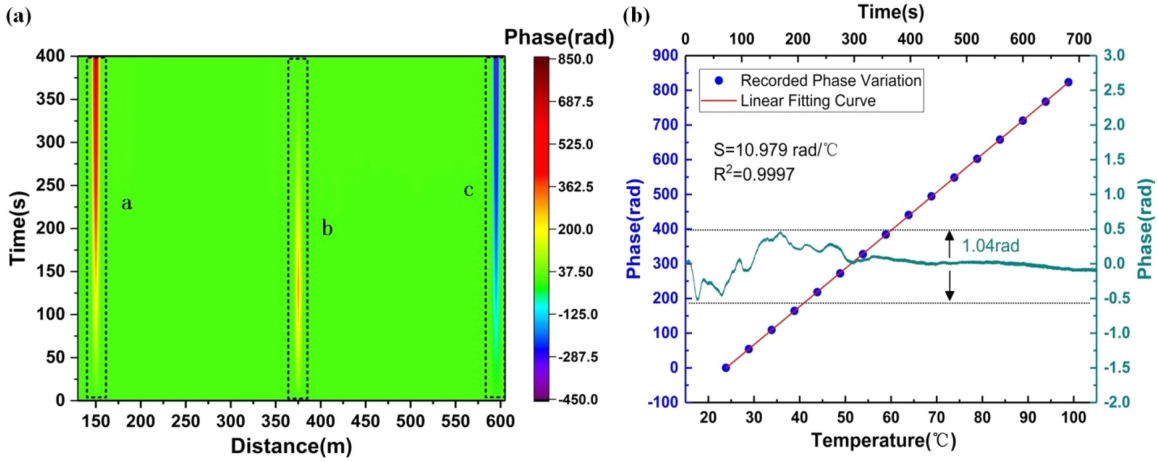

Fig. 7. (a) Temperature color map of phase variation along the sensing fiber. (b) Relationship between the phase variation and temperature change for 10 cm FUT and the recorded phase fluctuation of reference fiber.

around 0.095 °C for 10 cm FUT. Owing that the thermal fluctuation within the insulating box is much lower than the temperature precision of system, the maximum phase fluctuation of the isolated fiber segment is irrelevant to the thermal instability, which can be regarded as phase demodulation accuracy of the system during this period. According to Equation (5), the phase variation is linearly proportional to the length of FUT and temperature variation, so the longer sensing fiber length would have higher temperature sensitivity. To verify this, we further measure the temperature sensitivity of system with 3 m and 5 m long fiber under test (FUT) at the temperature range from 30 °C to 50 °C with 2 °C temperature increment. As shown in Fig. 8, the temperature sensitivity of 3 m FUT and 5 m FUT are 325.148 rad/°C and 536.273 rad/°C respectively, which are almost 30 times and 50 times higher than the one of 10 cm FUT. And the result is consistent with theoretical analysis. In addition, the temperature precision of the system can be improved to 0.002 °C with the 5 m FUT.

To demonstrate the fast temperature-responding speed of the system, we recorded both the temperature and the phase variation process of the 10 cm FUT simultaneously. Firstly, the temperature of thermal controller keeps 20 °C for 30 seconds. After that, we turn on the heating switch of the thermal controller and increase to 30 °C. The temperature of thermal controller has been increased

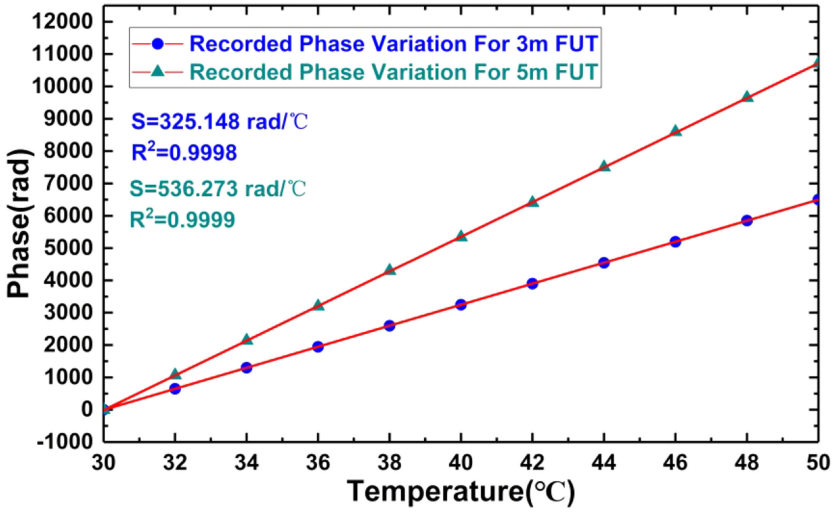

Fig. 8. The temperature sensitivity of 3 m FUT and 5 m FUT.

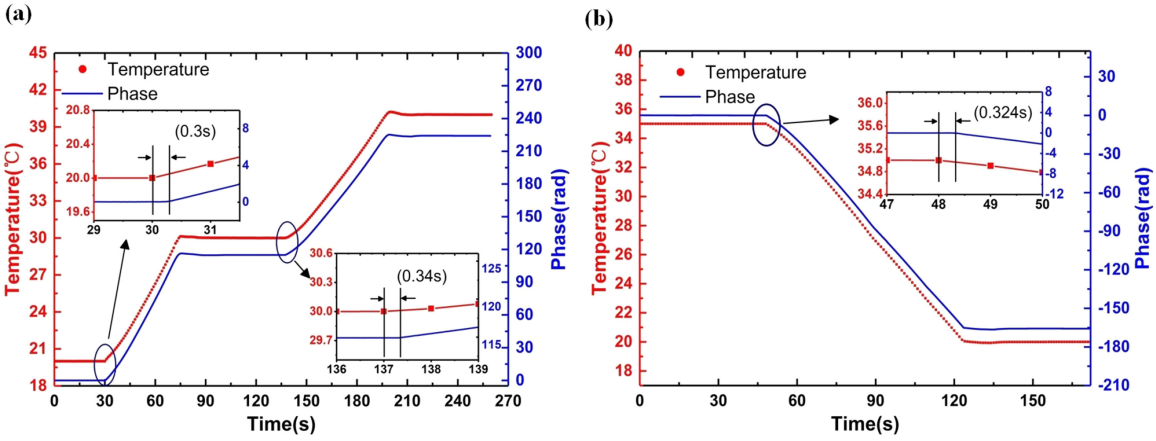

Fig. 9. (a) The curve of phase response to temperature rising and the recorded temperature every one second. (b) The curve of phase response to temperature decreasing and the recorded temperature every one second.

gradually and then held a temperature stabilization nearby 30 °C. Next, the thermal controller heats up again until its temperature is stable in the range of 40 °C ± 0.001 °C. Predictably, phase variation tendency of the FUT is identical with the temperature change as shown in Fig. 9(a). The two insets of Fig. 9(a) show the sensor has a response time of 0.3 seconds at 20 °C, and 0.34 at 30 °C. Furthermore, we tested the responding speed of temperature decreasing process. The temperature of FUT is increased and kept at 35 °C for a period of time and then decreased to 20 °C. The phase variation of the FUT varying with the temperature decreasing is illustrated in Fig. 9(b). A response time of 0.324 seconds to the external temperature decreasing can be obtained from the inset of Fig. 9(b). Consequently, we can confirm that the system has a fast-response to the external temperature change, with the response time of only about 0.3 seconds.

In particular, although the spatial resolution in this experiment is only 5 m, it can be further improved by changing the interval between adjacent BEPs. Besides, it can be seen that there is a tradeoff between the temperature sensitivity and the length of fiber disturbed by temperature change according to Equation (5), and hence the potential response range of the temperature can

be anticipated less than 1 cm, which is meaningful for the early warning of ultra-small sized fire source in the special oil and gas pipelines monitoring applications.

4. Conclusions

In conclusion, a wideband frequency and high precision distributed fiber sensor for simultaneous measurement of vibration and temperature is demonstrated. In order to enhance SNR and achieve high-precision phase measurement, integration of the BEOF and coherent phase detection is employed. Additionally, the wavelet packet decomposition algorithm is adopted to effectively discriminate the quasi-static temperature and dynamic vibration signals. The experimental results prove that the system has the capabilities of wide frequency bandwidth from 0.01 Hz to 20 kHz and high-fidelity waveform recovery. Besides, temperature variation applied on short fiber length of only 10 cm can be successfully detected with high precision of 0.095 °C and fast temperature-response speed approximately 0.3 seconds. Therefore, the sensor has great potential applications for the early warning of centimeters-level of the fire source in the special oil and gas pipelines monitoring.

References

[1] K. Miah and D. Potter, "A review of hybrid fiber-optic distributed simultaneous vibration and temperature sensing technology and its geophysical applications," *Sensors*, vol. 17, no. 11, 2017, Art. no. 2511.
[2] J. H. Hu *et al.*, "Strain-induced vibration and temperature sensing BOTDA system combined frequency sweeping and slope-assisted techniques," *Opt. Exp.*, vol. 24, no. 12, pp. 13610–13620, 2016.
[3] J. P. Dakin *et al.*, "Distributed optical fibre Raman temperature sensor using a semiconductor light source and detector," *Electron. Lett.*, vol. 21, no. 13, pp. 569–570, 1985.
[4] X. Bao and L. Chen, "Recent progress in Brillouin scattering based fiber sensors," *Sensors*, vol. 11, no. 4, pp. 4152–4187, Mar. 2011.
[5] L. Q. Luo *et al.*, "Frequency uncertainty improvement in a STFT-BOTDR using highly nonlinear optical fibers," *Opt. Exp.*, vol. 26, no. 4, pp. 3870–3881, Feb. 2018.
[6] X. P. Zhang *et al.*, "A high performance distributed optical fiber sensor based on Φ-OTDR for dynamic strain measurement," *IEEE Photon. J.*, vol. 9, no. 3, Jun. 2017, Art. no. 6802412.
[7] G. Yang, X. Fan, S. Wang, B. Wang, Q. Liu, and Z. He, "Long-range distributed vibration sensing based on phase extraction from phase-sensitive OTDR," *IEEE Photon. J.*, vol. 8, no. 3, Jun. 2016, Art. no. 6802412.
[8] F. Zhu, Y. Zhang, L. Xia, X. Wu, and X. Zhang, "Improved Φ-OTDR sensing system for high-precision dynamic strain measurement based on ultra-weak fiber Bragg grating array," *J. Lightw. Technol.*, vol. 33, no. 23, pp. 4775–4780, Dec. 2015.
[9] J. D. Zhang *et al.*, "High spatial resolution distributed fiber system for multi-parameter sensing based on modulated pulses," *Opt. Exp.*, vol. 24, no. 24, pp. 27482–27493, Nov. 2016.
[10] Y. Muanenda *et al.*, "Hybrid distributed acoustic and temperature sensor using a commercial off-the-shelf DFB laser and direct detection," *Opt. Lett.*, vol. 41, no. 3, pp. 587–590, Feb. 2016.
[11] Y. Koyamada, M. Imahama, K. Kubota, and K. Hogari, "Fiber-optic distributed strain and temperature sensing with very high measurand resolution over long range using coherent OTDR," *J. Lightw. Technol.*, vol. 27, no. 9, pp. 1142–1146, May 2009.
[12] X. Lu *et al.*, "Temperature-strain discrimination in distributed optical fiber sensing using phase-sensitive optical time-domain reflectometry," *Opt. Exp.*, vol. 25, no. 14, pp. 16059–16071, Jul. 2017.
[13] H. Li *et al.*, "Coherent OTDR based ultra-high sensitive acoustic sensor assisted with distributed microstructured optical fiber (DMOF) and hollow cylinder transducer," in *Proc. IEEE/AIT Int. Conf. Adv. Infocomm Technol.*, 2018, pp. 1–4.
[14] Y. Lu, T. Zhu, L. Chen, and X. Bao, "Distributed vibration sensor based on coherent detection of phase-OTDR," *J. Lightw. Technol.*, vol. 28, no. 22, pp. 3243–3249, Nov. 2010.
[15] Y. K. Dong *et al.*, "Quantitative measurement of dynamic nanostrain based on a phase-sensitive optical time domain reflectometer," *Appl. Opt.*, vol. 55, no. 28, pp. 7810–7815, Oct. 2016.
[16] L. Zhou *et al.*, "Distributed strain and vibration sensing system based on phase-sensitive OTDR," *IEEE Photon. Technol. Lett.*, vol. 27, no. 17, pp. 1884–1887, Sep. 2015.
[17] S. P. Nikitin *et al.*, "Distributed temperature sensor based on a phase-sensitive optical time-domain Rayleigh reflectometer," *Laser Phys.*, vol. 28, no. 8, 2018, Art. no. 085107.